ELSEVIER

Journal of Photochemistry and Photobiology A: Chemistry 148 (2002) 5–10

Journal of Photochemistry and Photobiology A:Chemistry

www.elsevier.com/locate/jphotochem

Modulating interfacial electron transfer dynamics in dye sensitised nanocrystalline metal oxide films

James R. Durrant*

Centre for Electronic Materials and Devices, Department of Chemistry, Imperial College, Exhibition Road, London SW7 2AY, UK

Received 24 July 2001; received in revised form 25 September 2001; accepted 25 September 2001

Abstract

The efficient generation of a stable charge separated state is fundamental to the performance of dye sensitised photoelectrochemical solar cells. In this paper we consider the parameters influencing the kinetics of electron injection and recombination. Our recent experimental data on these processes is reviewed and compared to data expected for simple homogeneous kinetic models. For both charge injection and recombination, such simple models are insufficient to explain experimental observations. The implications of this observation are discussed and possible alternative models reviewed. © 2002 Elsevier Science B.V. All rights reserved.

Keywords: Interfacial electron transfer; Dye sensitisation; Solar cell; Nanocrystalline

1. Introduction

Interfacial electron transfer kinetics are critical to the function of dye sensitised solar cells [1]. These different electron transfer reactions are summarised in Fig. 1. Efficient charge separation requires the electron injection kinetics (k_{inj}) to be faster than decay of the excited state decay to ground (k_0). Efficient cation transfer to the redox electrolyte (k_{RR}) requires the dye cation re-reduction by the redox couple to be faster than recombination between injected electrons and photogenerated dye cations (k_{cr1}). Efficient charge collection requires charge recombination between injected electrons and oxidised redox species in the electrolyte (k_{cr2}) to be slower than transport of the these species to the SnO_2 electrodes and counter-electrodes, respectively. In this paper we will address some of the parameters influencing these dynamics, focusing particularly upon the electron injection and recombination processes k_{inj} and k_{cr1} observed following pulsed laser excitation of the dye sensitised nanocrystalline TiO_2 films:

$$D^* \xrightarrow{k_{inj}} D^+ + e^-_{M.O.} \quad (1)$$

$$D^+ + e^-_{M.O.} \xrightarrow{k_{cr1}} D \quad (2)$$

From (1) it is apparent that the electron injection should ideally exhibit first order, exponential kinetics. Similarly from (2), second order dynamics should in general be expected for the recombination reaction k_{cr1}. However we note that the density of electrons $[e^-_{M.O.}]$ may result not only from photoinjected electrons but also the density of electrons present in the metal oxide conduction band/sub-bandgap states prior to optical excitation, as defined by the position of the metal oxide Fermi level. The metal oxides under consideration here are n-type semiconductors. In the limit of low intensity optical excitation and therefore a low density of photogenerated dye cations, the total electron density will be greater than the density of photogenerated dye cations ($[e^-_{M.O.}] \gg [D^+]$); under such conditions pseudo-first order recombination dynamics are expected.

Following theoretical treatments of interfacial electron transfer processes developed in the 1960s, the rate constant k_{inj} for electron injection from the excited state of an adsorbed dye molecule into the conduction band of an electrode can be expressed as [2]:

$$k_{inj} = A \int V^2 (1 - f(E, E_F)) g(E) \exp \times \left(\frac{-(E_m - E + \lambda)^2}{4\lambda k_B T} \right) dE \quad (3)$$

where k_{inj} is the electron injection rate constant, V the electronic coupling between the dye excited state and each conduction band state of the electrode (assumed to be state

* Tel.: +44-20-7594-5321; fax: +44-20-7594-5801.
E-mail address: j.durrant@ic.ac.uk (J.R. Durrant).

PII: S1010-6030(02)00071-0

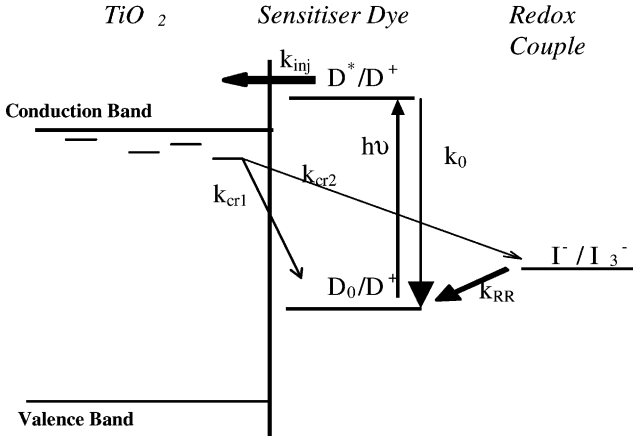

Fig. 1. Schematic diagram showing the different interfacial electron transfer processes: injection from dye excited state into conduction band of semiconductor (k_{inj}); regeneration of the dye cation by electron transfer from the redox couple (k_{RR}); recombination of electron with the dye cation (k_{cr1}); electron recombination to the redox couple (k_{cr2}) and excited state decay to ground (k_0).

independent) and E_m the excited state oxidation potential energy of the adsorbed molecule. E is the electrochemical potential energy of conduction band states (and therefore negative for most semiconductors). The equation corresponds essentially to an extension of Marcus non-adiabatic electron transfer theory by incorporating a continuum of electronic states in the semiconductor. $g(E)$ is the normalised density of states of these electronic states, $f(E,E_F)$ is the Fermi occupancy factor to account of the fact that electron injection is only possible into unoccupied states. λ is the reorganisational energy associated with electron injection. The exponential term in this equation results in electron injection occurring optimally to conduction band states lying λ below the dye excited state energy, corresponding to activationless electron injection. A central prediction of this equation is that as the Fermi level (or conduction band edge) of the semiconductor is raised to an energy within $\sim\lambda$ of the dye excited state oxidation potential, the rate of electron injection is retarded. This retardation arises from the reduction in the number of unoccupied acceptor states available for electron injection. An analogous treatment can be made for the recombination reaction k_{cr1} [2]. Such recombination reactions have been previously reported to lie in the Marcus inverted region, with a significant activation barrier to recombination.

The dynamics of electron injection [3–12] and charge recombinational [3–16] have received extensive experimental study in recent years. In this paper, we review some of our own studies of these dynamics and consider the extent to which they are consistent the simple non-adiabatic electron transfer theory as detailed in Eqs. (1)–(3) above. We address in particular the behaviour of nanocrystalline TiO_2 films sensitised by the dye ruthenium(II)*cis*-(2,2′-bipyridyl-4,4′-dicarboxylate)$_2$(NCS)$_2$ (Ru(dcbpy)$_2$(NCS)$_2$), a dye/semiconductor combination of particular interest for the commercial development of dye sensitised solar cells [17].

2. Materials and methods

Transparent nanocrystalline anatase TiO_2 films (average particle diameter of 15 nm and film thickness of 8 μm) were prepared as reported previously [10,13]. These films were sensitised with Ru(dcbpy)$_2$(NCS)$_2$ by immersion in acidified ethanol dye solutions at room temperature overnight. Sensitised films were studied either covered by a drop of 50:50 propylene carbonate:ethylene carbonate (PC/EC) under a glass cover slide or incorporated as the working electrode of a three electrode photoelectrochemical cell. Details of the experimental apparatus employed for the transient absorption experiments are given in detail elsewhere [10,13]. For all such experiments, the intensity of the excitation pulses was attenuated to ensure excitation densities of <1 absorbed photon per nanoparticle.

3. Results and discussion

3.1. TiO_2 density of states

The form of the TiO_2 density of states $g(E)$ is critical to evaluation of Eq. (3). A key consideration in experimental determination of $g(E)$ is that, due to the small diameter (approximately 15 nm) of the metal oxide nanoparticles comprising the film, $g(E)$ is strongly dependent upon the adsorption of charged species to the film surface. In particular, due to the protonation/deprotonation of surface bound hydroxyl groups, nanocrystalline TiO_2 films have been shown to exhibit Nernstein shifts of their conduction band energetics by 60 meV per pH unit [18]. Potential determining ions for the flat band potential of such films have been shown to include not only protons but also small metal cations such as lithium [19]. Experimental probes of $g(E)$ in the presence of electrolytes have been largely limited to electrochemical and spectroelectrochemical studies of electron density [$e^-_{M.O.}$] as a function of applied potential. Such experiments have, for example, exploited the characteristic blue/black coloration of nanocrystalline TiO_2 films at negative potentials attributed to the reduction of Ti^{4+} ions to Ti^{3+}. Such studies have typically found that the electron density increases approximately exponentially with negative applied potential E_F:

$$[e^-_{M.O.}] \propto \exp\left(-\frac{E_F}{E_0}\right) \quad (4)$$

Typical experimental values for E_0 lie in the range 60–100 meV [20–22]. Assuming that $g(E)$ is independent of E_F, the observation that $E_0 > k_BT$ suggests these electrons do not primarily result from increased occupancy of the TiO_2 conduction band. This behaviour is however consistent with an exponentially increasing density of states:

$$g(E) \propto \exp\left(-\frac{E}{E_0}\right) \quad (5)$$

It has thus been suggested that nanocrystalline TiO_2 films exhibit an exponential tail of sub-bandgap states below their conduction band. These states are typically assigned to localised Ti^{3+} species.

3.2. Electron injection

Efficient charge separation requires the rate of electron injection to be faster than the decay of the dye excited state to ground. Following optical excitation of the main metal-to-ligand charge transfer transition of $Ru(dcbpy)_2(NCS)_2$ (absorption maximum ~540 nm) in solution, a rapid relaxation (<150 fs) of this excited state results in the generation of a lower energy excited state [3], thought to be of primarily triplet character, with a emission maximum at ~800 nm. Such behaviour is typical of ruthenium bipyrdyl dyes [23]. The lifetime of this excited state is 50 ns in degassed solvent [17], and 3–25 ns when absorbed to an inert substrate (ZrO_2) [3]. The kinetics of electron injection for this dye can be monitored by the red shift of a photoinduced absorption maximum from ~720 nm for the dye excited state to 800 nm for the dye cation [3].

For $Ru(dcbpy)_2(NCS)_2$ sensitised TiO_2 films covered in an inert solvent (PC/EC), non-exponential kinetics are observed on timescales from <150 fs to tens or hundreds of picoseconds. In our own studies, multiexponential analyses of such data have resolved components assigned to electron injection with lifetimes (relative amplitudes) of <100 fs (0.29), 1.0 ps (0.25) and 13 ps (0.46) [4,10]. Similar experiments reported elsewhere resolved similar components, with the addition of a further component with lifetime of 100 ps [11]. Remarkably similar, multiexponential injection kinetics have been reported for a range of other sensitiser dyes adsorbed to nanocrystalline TiO_2 films, including zinc and free base tetracarboxyphenyl porphyrins (Zn and H_2 TCPP, respectively) [4] and fluorescin 27 [9]. We note that all of these dyes are expected to have excited state energies well above the TiO_2 conduction band edge and be bound such that the excited state is close to the TiO_2 surface. Studies of sensitiser dyes, employing for example, spacers between the dye excited state and the film surface have reported a significant retardation of the injection kinetics [24].

The non-exponential nature of the injection kinetics are clearly inconsistent with homogeneous, first order injection kinetics as expressed by Eq. (1). This non-exponentiality is not dye specific and therefore cannot be attributed to kinetic competition between electron injection and relaxation dynamics of the dye excited state. (Such kinetic competition has been observed to be significant where the dye excited state is too low in energy for rapid electron injection [7].) We have proposed elsewhere [12] that this non-exponential behaviour may derive from local inhomogeneities in density of acceptor states $g(E)$:

$$g_i(E) = g(E + d_i) \quad (6)$$

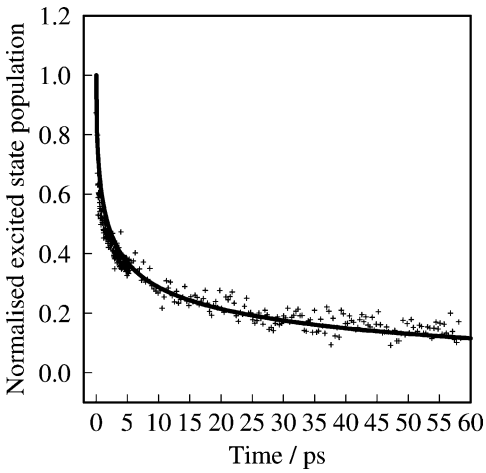

Fig. 2. Comparison of experimental electron injection kinetics (+) with model calculations (—) employing the inhomogeneous model with $\Delta/E_0 = 1.5$. Data obtained from transient absorption data for $Ru(dcbpy)_2(NCS)_2/TiO_2$ films (+) covered in PC/EC. The absolute excited state populations were determined from comparison of transient absorption and emission data as detailed in Ref. [12].

where the local density of states $g_i(E)$ of site i exhibits an energetic shift from the ensemble averaged density of states by an energy shift d_i. Shifts of the energetics of $g(E)$ have been suggested elsewhere to be the origin of variations in the yield [15] and kinetics [10] of electron injection for similar dye sensitised TiO_2 films as a function of the concentration of potential determining ions in the electrolyte in which the film is immersed. Microscopically, local variations in surface charge will result in inhomogeneities in the density of acceptor states $g_i(E)$ for each dye molecule, as indicated in Eq. (6). Fig. 2 shows a comparison of numerical calculations using Eq. (3) and employing this inhomogeneous model with experimental injection data. The model calculations employs an exponential density of states as given in Eq. (5) and a Gaussian distribution of d_i with FWHM Δ. The non-exponential shape of the model calculations was determined by the value of the ratio Δ/E_0, with $\Delta/E_0 = 1.5$ providing the best fit to the data. Using a value of E_0 of 100 meV, typical of recent experimental observations, this yields a value of $\Delta = 150$ meV. This magnitude of inhomogeneous broadening seems reasonable being, for example, of similar magnitude to the energetic distribution of chlorine radical pairs reported for photosynthetic reaction centres [25,26]. The energetic distribution observed in such pigment/protein complexes has also attributed to inhomogeneities in the charge environment of individual pigments due to protonation/deprotonation of neighbouring groups (in this case amino acids rather than surface bound hydroxy groups). The presence of local inhomogeneities is moreover consistent with single molecule emission studies of cresyl violet sensitised ITO films, which indicated an inhomogeneous distribution of injection kinetics [27].

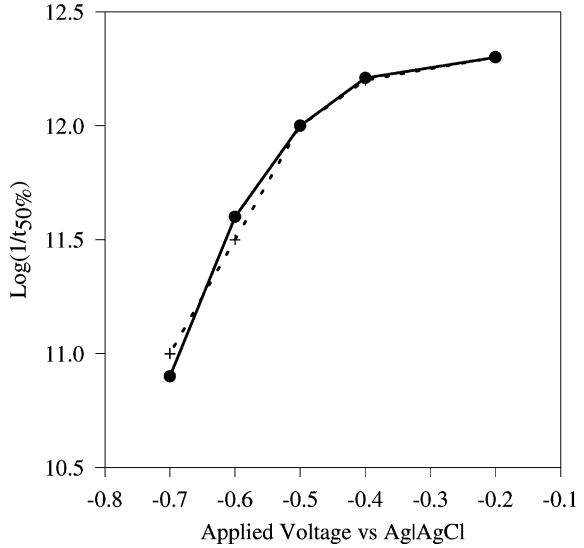

Fig. 3. Comparison of the electrical potential dependence of the half time for electron injection, $t_{50\%}$, observed experimentally (+) with that calculated from non-adiabatic electron transfer theory as given by Eq. (3) (●). Experimental data were obtained for a $Ru(dcbpy)_2(NCS)_2$ sensitised TiO_2 film in an MeCN/tetrabutyl ammonium perchlorate electrolyte. The best fit to the experimental data, as shown (●) yielded fitting parameters of $E_m = -0.75 \pm 0.05$ V versus Ag/AgCl and $\lambda = 0.25 \pm 0.05$ eV. Reproduced from Ref. [10].

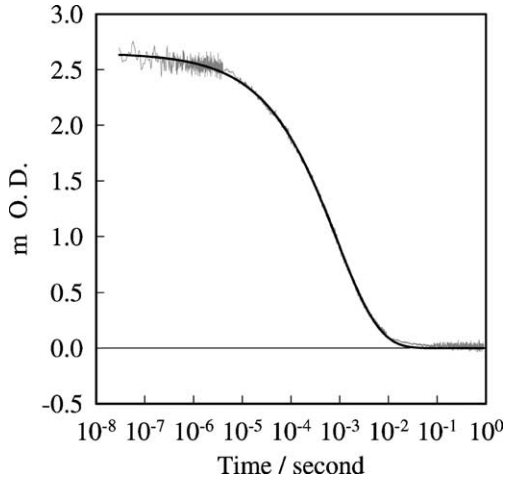

Fig. 4. Charge recombination dynamics for $Ru(dcbpy)_2(NCS)_2/TiO_2$ films covered in PC/EC, monitored by the decay of the dye cation absorption band at 800 nm. The smooth line is the best fit to the data employing a stretched exponential (Eq. (7)), with fit parameters of $\tau = 0.9\,\mu s$ and $\alpha = 0.5$. Adapted from Ref. [3].

Following Eq. (3), the rate of electron injection is expected to be retarded as the Fermi level of the TiO_2 is raised, as acceptor states for electron injection become occupied. Fig. 3 shows a comparison of experimental data with model calculations addressing this issue. Data were collected in a three electrode photoelectrochemical cell, in which the sensitised film comprised the working electrode [10]. Modulation of the potential applied to this electrode relative to the Ag/AgCl reference electrode results in modulation of the TiO_2 Fermi level. In these experiments a full kinetic analysis of the injection dynamics was not possible as sufficient signal averaging was prevented by the limited stability of the sensitiser dye at negative potentials. Our analysis is therefore limited to consideration of the half time for electron injection ($t_{50\%}$) upon applied bias. It is apparent that the application of negative potentials results in a retardation of the injection kinetics by up to a factor 25. Model calculations employing Eq. (3) were found not to be sensitive to the value of E_0 employed for $E_0 \geq 100$ meV. Such calculations provided a good fit to the experimental data with a value for the reorganisational energy $\lambda = 0.25 \pm 0.05$ eV.

3.3. Recombination dynamics

Following electron injection into the TiO_2 film, the resulting charge separated state $D^+\ e^-_{M.O.}$ is remarkably stable. Under the same experimental conditions as those employed in Fig. 2, the half time for charge recombination ($t_{50\%}$) is 0.4 ms. As for the injection kinetics, the recombination kinetics are non-exponential. They can be reasonably fitted to a stretched exponential:

$$\Delta OD \propto \exp\left(-\left(\frac{t}{\tau}\right)^{\alpha}\right) \quad (7)$$

as illustrated in Fig. 4. Values of α obtained from such fits range from 0.25 to 0.5 dependent upon the electrolyte employed.

Following Eq. (2), the recombination dynamics are expected to be first order in electron density $[e^-_{M.O.}]$. Experimental studies have indeed confirmed a strong dependence of the recombination dynamics upon electron density [13]. Studies in which $[e^-_{M.O.}]$ was increased by the application of a negative potential to the TiO_2 electrode resulted in rapid acceleration of the recombination kinetics. Shifting the applied potential from +0.1 V versus Ag/AgCl to −0.8 V resulted in an acceleration of recombination half time, $t_{50\%}$, by $\sim 10^8$ from 1 ms to ~3 ps. Similarly studies conducted at a constant applied potential, but in which $[e^-_{M.O.}]$ was modulated by employing different electrolyte solutions to vary $g(E)$, resulted in variations in $t_{50\%}$ by up to 10^6. However these dependencies are too large to be consistent with a first order dependence of $t_{50\%}$ upon $[e^-_{M.O.}]$. The lower limit for $[e^-_{M.O.}]$ in these experiments observed, for example, at positive applied potentials, is the electron density generated by the laser pulse, corresponding to approximately one electron per nanoparticle. A linear dependence of recombination rate upon electron density would therefore require electron densities of up to 10^8 per nanoparticle, which is clearly implausible. We further note that as the recombination process is thought to occur in the Marcus inverted region ($|\Delta G| > \lambda$), a more detailed consideration including integration over all occupied TiO_2 states would result in a

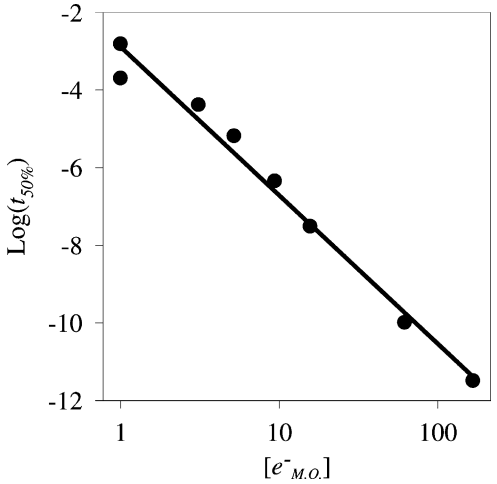

Fig. 5. Plot of the electron density [$e^-_{M.O.}$] against the half time for charge recombination $t_{50\%}$ observed for a $Ru(dcbpy)_2(NCS)_2$ sensitised TiO_2 film in an ethanol/tetrabutyl ammonium perchlorate electrolyte. The electron density was modulated by varying the potential applied to the TiO_2 electrode in a three electrode photoelectrochemical cell. Electron densities were determined spectroelectrochemically in the absence of absorbed dyes. Recombination half times were determined by transient absorption spectroscopy. Adapted from Refs. [13,14].

sub-linear dependence of $t_{50\%}$ upon [$e^-_{M.O.}$], in even greater contrast with the experimental observations.

Fig. 5 shows a quantitative analysis of the dependence of the half time for charge recombination, $t_{50\%}$, upon electron density [$e^-_{M.O.}$]. For this plot [$e^-_{M.O.}$] was determined independently by spectroelectrochemical studies of steady state film optical density as a function of applied potential, employing the characteristic Ti^{3+} absorption associated with $e^-_{M.O.}$ in TiO_2. It is apparent that $t_{50\%}$ exhibits a power law dependence upon [$e^-_{M.O.}$]:

$$t_{50\%} \propto [e^-_{M.O.}]^{-\beta} \quad (8)$$

where $\beta = 2$–4 dependent upon the electrolyte employed. This behaviour is clearly inconsistent with a simple rate law first order in [$e^-_{M.O.}$].

It has recently been shown that these experimental observations are consistent with a model in which the recombination process is primarily controlled not by the rate of interfacial electron transfer as expressed by Eq. (3), but by the dynamics of electron transport within the TiO_2 electrode [14,28]. The model, developed from the continuous time random walk model of Scher and Montroll [29], is based upon a random walk of electron between an energetic distribution of trap sites in the film. Each step of the random walk requires thermal excitation of the trapped electron up to the conduction band and therefore is dependent upon the trap depth. The non-linear dependence of the recombination kinetics upon [$e^-_{M.O.}$] results from the increased mobility of the electrons as the film Fermi level is raised, as increasingly shallow trap become occupied. The model furthermore predicts that, for an exponential density of states, the fitting

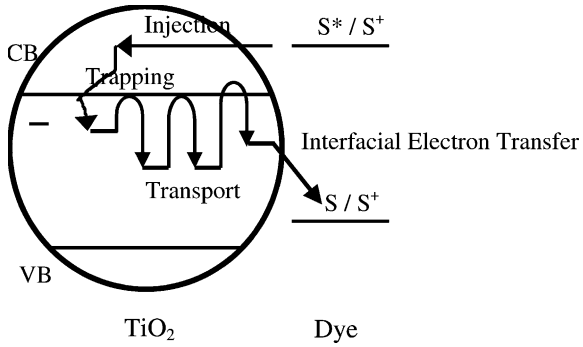

Fig. 6. Illustration of model of electron injection and charge recombination in dye sensitised nanocrystalline TiO_2 films.

parameters α and β of Eqs. (7) and (8) obtained from analyses of experimental data for different electrolytes should be related by

$$\alpha = \frac{1}{\beta} \quad (9)$$

This correlation is in good agreement with experimental observations for a range of different electrolytes, providing further support for the validity of this model.

3.4. A model of interfacial electron transfer dynamics

A model of the interfacial dynamics consistent with the experimental observations discussed above is illustrated in Fig. 6. Following optical excitation of the $Ru(dcbpy)_2(NCS)_2$ sensitiser dye, an electron is injected from the dye excited state into acceptor states of the semiconductor. The non-exponential kinetics observed this process, and their dependence upon TiO_2 Fermi level, are consistent with non-adiabatic electron transfer theory. The injection proceeds primarily on timescales slower than relaxation of the dye excited state. The half time for electron injection is, in the absence of applied bias, ~0.4 ps, although the injection kinetics are non-exponential, with a significant proportion occurring on timescales >100 ps.

Following electron injection, the electron relaxes to localised sub-bandgap states associated with Ti^{3+} formation. Subsequent charge recombination requires thermal detrapping of this electron and motion through the TiO_2 film until it is sufficiently close to an oxidised dye molecule such that the direct electron transfer is possible. The initially injected electron does not appear to remain adjacent or associated with its corresponding dye cation as the recombination dynamics are controlled by the total density of electrons in the film, with electrons injected by electrical bias and optical photoinjection yielding similar recombination behaviour. The electron motion within the TiO_2 film can be well described by the CTRW model, corresponding to anomalous diffusion of electrons through an energetic distribution of trap sites.

Acknowledgements

The author would like to thank his co-workers for many useful and helpful discussions, including in particular Jenny Nelson, Saif Haque, Yasuhiro Tachibana and David Klug. Financial support from the EPSRC is very grateful acknowledged.

References

[1] A. Hagfeldt, M. Gratzel, Acc. Chem. Res. 33 (2000) 269–277.
[2] W. Schmickler, Interfacial Electrochemistry, Oxford University Press, Oxford, 1996.
[3] Y. Tachibana, J.E. Moser, M. Grätzel, D.R. Klug, J.R. Durrant, J. Phys. Chem. 100 (1996) 20056–20062.
[4] Y. Tachibana, S.A. Haque, I.P. Mercer, D.R. Klug, J.R. Durrant, J. Phys. Chem. B 104 (2000) 1198–1205.
[5] B. Burfeindt, T. Hannappel, W. Storck, F. Willig, J. Phys. Chem. 100 (1996) 16463–16465.
[6] J.B. Asbury, R.J. Ellingson, H.N. Ghosh, S. Ferrere, A.J. Nozik, T. Lian, J. Phys. Chem. B 103 (1999) 3110–3119.
[7] S. Iwai, K. Hara, S. Murata, R. Katoh, H. Sugihara, H. Arakawa, J. Chem. Phys. 113 (2000) 3366–3373.
[8] R. Huber, S. Spörlein, J.E. Moser, M. Grätzel, J. Wachtveitl, J. Phys. Chem. B 104 (2000) 8995–9003.
[9] G. Benkö, M. Hilgendorff, A.P. Yartsev, V. Sundström, J. Phys. Chem. B 105 (2001) 967–974.
[10] Y. Tachibana, S.A. Haque, I.P. Mercer, J.E. Moser, D.R. Klug, J.R. Durrant, J. Phys. Chem. B 105 (2001) 7428–7431.
[11] J. Kallioinen, V. Lehtovuori, P. Myllyperkiö, J. Korppi-Tommola, Chem. Phys. Lett. 340 (2001) 217–221.
[12] Y. Tachibana, I.V. Rubstov, I. Montanari, K. Yoshihara, D.R. Klug, J.R. Durrant, J. Photochem. Photobiol. A 142 (2001) 215–220.
[13] S.A. Haque, Y. Tachibana, R. Willis, J.E. Moser, M. Grätzel, D.R. Klug, J.R. Durrant, J. Phys. Chem. B 104 (2000) 538–547.
[14] J. Nelson, S.A. Haque, D.R. Klug, J.R. Durrant, Phys. Rev. B 63 (2001) 5321–5329.
[15] C.A. Kelly, F. Farzad, D.W. Thompson, J.M. Stipkala, G.J. Meyer, Langmuir 15 (1999) 7047–7054.
[16] P.V. Kamat, I. Bedja, S. Hotchandani, L.K. Patterson, J. Phys. Chem. 100 (1996) 4900–4908.
[17] M.K. Nazeeruddin, A. Kay, I. Rodicio, R. Humphry-Baker, E. Muller, P. Liska, N. Vlachopoulos, M. Grätzel, J. Am. Chem. Soc. 115 (1993) 6382–6390.
[18] G. Rothenberger, D. Fitzmaurice, M. Grätzel, J. Phys. Chem. 96 (1992) 5983–5986.
[19] G. Redmond, D. Fitzmaurice, J. Phys. Chem. 97 (1993) 1426–1430.
[20] N.W. Duffy, L.M. Peter, R.M.G. Rajapakse, K.G.U. Wijayantha, Electrochem. Commun. 2 (2000) 658–662.
[21] R.L. Willis, C. Olson, B. O'Regan, T. Lutz, J. Nelson, J.R. Durrant, submitted to J. Phys. Chem. B.
[22] A. Kay, M. Grätzel, J. Phys. Chem. 97 (1993) 6272–6277.
[23] N.H. Damrauer, G. Cerullo, A. Yeh, T.R. Boussie, C.V. Shank, J.K. McCusker, Science 275 (1997) 54–57.
[24] J.B. Asbury, E. Hao, W. Wang, Lian, J. Phys. Chem. B 104 (2000) 11957–11964.
[25] M.-L. Groot, E.J.G. Petermann, P.J.M. vanKan, I.H.M. vanStokkum, J.P. Dekker, R. vanGrondelle, Biophys. J. 67 (1994) 318–330.
[26] A. Ogrodnik, W. Keupp, M. Volk, G. Aumeier, M.E. Michelbeyerle, J. Phys. Chem. 98 (1994) 3432–3439.
[27] H.P. Lu, X.S. Xie, Z. Phys. Chem. 212 (1999) 59–66.
[28] J. Nelson, Phys. Rev. B 59 (1999) 15374–15380.
[29] H. Scher, E.W. Montroll, Phys Rev. B 12 (1975) 2455.